JOC The Journal of Organic Chemistry

Article

N,O #-Conjugated 4-Substituted-1,3-Thiazole BF2 Complexes: Synthesis and Photophysical Properties

Mykhaylo A. Potopnyk, Roman Lytvyn, Yan Danyliv, Magdalena Ceborska, Oleksandr Bezvikonnyi, Dmytro Volyniuk, and Juozas Vidas Grazulevicius

J. Org. Chem., **Just Accepted Manuscript** • DOI: 10.1021/acs.joc.7b02239 • Publication Date (Web): 04 Jan 2018

Just Accepted

ACS Publications

The Journal of Organic Chemistry is published by the American Chemical Society.
1155 Sixteenth Street N.W., Washington, DC 20036

N,O π-Conjugated 4-Substituted-1,3-Thiazole BF_2 Complexes: Synthesis and Photophysical Properties

Mykhaylo A. Potopnyk,*,† Roman Lytvyn,‡,# Yan Danyliv,‡ Magdalena Ceborska,§ Oleksandr Bezvikonnyi,‡ Dmytro Volyniuk,‡ and Juozas Vidas Gražulevičius*,‡

†Institute of Organic Chemistry, Polish Academy of Sciences, Kasprzaka 44/52, 01-224, Warsaw, Poland, e-mail: potopnyk@gmail.com

‡Department of Polymer Chemistry and Technology, Kaunas University of Technology, Radvilenu pl. 19, LT-50254 Kaunas, Lithuania

#Department of Organic Chemistry, Ivan Franko National University of Lviv, Kyryla and Mefodia St. 6, 79005 Lviv, Ukraine

§Institute of Physical Chemistry, Polish Academy of Sciences, Kasprzaka 44/52, 01-224, Warsaw, Poland

Abstract: A series of 1,3-thiazole based organoboron complexes have been designed and synthesized by acylation of 2-amino-4-subsituted-1,3-thiazoles with (4-dimethylamino)benzoyl chloride, and the subsequent BF_2 complexation reaction. The influence of substituents in position 4 of the thiazole ring on photophysical properties of the complexes has been investigated. Synthesized thiazolo[3,2-c][1,3,5,2]oxadiazaborinines mainly showed intensive fluorescence in solutions. Complex with 4,5-unsubstituted thiazole unit demonstrated aggregation induced emission (AIE) effect and very high fluorescent quantum yield (94%) in the solid state, because of the inhibition of π−π/π−n interactions in the molecular packing.

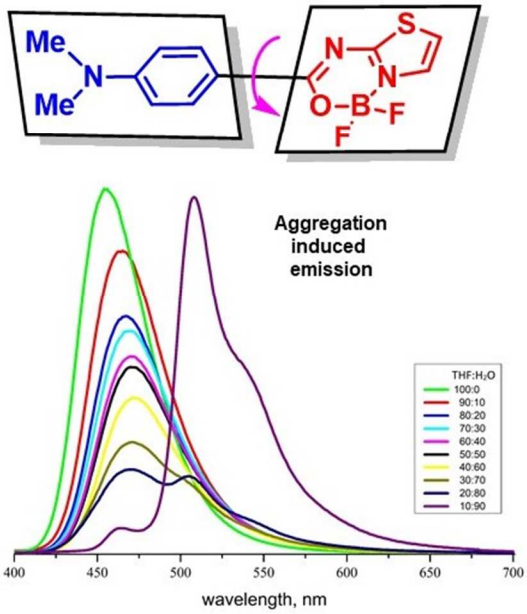

Introduction

The evolution of new technologies entails an intensive scientific research in the area of photo- and electroactive organic materials. The development of luminescent compounds, which can serve as components of various optoelectronic devices such as organic light-emitting diodes

(OLEDs)[1-5] or light-emitting electrochemical cells (OLECs),[6,7] optical sensing materials in biological[8-10] and supramolecular[11-13] systems is one of the biggest scientific challenges.

In this context, organoboron complexes have many advantages compared to other fluorophores (porphyrins, metal complexes, etc.) including strong absorption bands in UV and visible regions, high fluorescent quantum yields, photostability, relatively long excited-state lifetime (1–5 ns), good solubility in common organic solvents; insensitivity to the environment e.g. pH.[14] Currently, the most investigated organoboron compounds are boron-dipyrromethene (BODIPY) derivatives.[15,16] Unfortunately, despite the intensive fluorescence of BODIPY dyes in solution, their emission in the solid state is usually weak, which limits optoelectronic applications.[17]

In the last few years, a study of different boron (III) organic complexes, including other than pyrrole heterocyclic units, was the subject of great research interest.[17] They are very attractive because of their optical variability and synthetic convenience. However, in contrast to boron complexes with *N*,*N*-chelating ligands,[18-25] *N*,*O*-analogues were little investigated. Mainly those based on phenolic[26-37] or *β*-ketoiminate[38-43] ligands were reported, while the complexes formed from amid group containing ligands are presented only as pyridine and 1,8-naphthyridine derivatives.[18,43-47] The use of *N*,*O* *π*-conjugated ligands with carbonyl *O*- and heterocyclic *N*-coordinating centers can opens the way to obtain various new boron (III) complexes with interesting properties. The design of the donor-acceptor type systems can lead to attractive electronic properties, such as chromism, charge transporting properties, *π*-conjugated electronic states recombination.[48-50]

In this article we report on the synthesis and photophysical properties of thiazolo[3,2-c][1,3,5,2]oxadiazaborinine derivatives.

Results and Discussion

Synthesis of Boron Complexes

Our strategy involves the incorporation of electron donating and accepting groups into the complex structure, which is anticipated to result in a donor-acceptor system. We have chosen 2,2-difluoro-1,3,5,2-oxadiazaborinine unit as previously known acceptor.[43-47] On the other hand, 4-dimethylaminophenyl group has been used as effective donor. To investigate the influence of substituents at the position 4 of the thiazole ring on photophysical properties of these boron dyes, we designed compounds with corresponding groups.

In order to realize this idea, we developed a simple synthetic way for the preparation of such complexes. 4-*R*-thizol-2-amines were selected as useful building blocks for construction the complexes. Unsubstituted thiazol-2amine (**2a**) is commercial available. 4-Methylthiazol-2-amine (**2b**) was prepared by reaction between acetone (**1b**), iodine, and thiourea in 37% yield. The other 4-*R*-thizol-2-amines (**2c–g**) were obtained by the Hantzsch thiazole reaction of 2-bromoketones (**1c–g**) with thiourea in 68–97% yields. To prepare the *N*,*O* ligands, 4-substituted thiazol-2-amines **2a–g** were acylated by (*para*-dimethylamino)benzoyl chloride **3** in the basic conditions in refluxing 1,4-dioxane to provide amides **4a–g** in 46–80% yields. Ligands **4a–g** were transformed into boron complexes **5a–g** by the treatment with boron trifluoride in the presence of diisopropylethylamine (DIPEA) in fair to good (48−77%) yields (Scheme 1). Such obtained complexes have different substitutes at position 4 of the thiazole ring, including donor and acceptor groups. All the synthesized compounds were characterized by high-resolution mass spectrometry and the IR and NMR analysis (^{1}H and ^{13}C for amines **2b–g** and ligands **4a–g**; and ^{1}H, ^{13}C, and ^{19}F for complexes **5a–g**). In addition, the structures of **5a** and **5c–e** were further confirmed by single-crystal X-ray analysis (Figure 1–4 and Tables S1–S4 in the Supporting Information).

Scheme 1. Synthesis of Complexes 5a–g

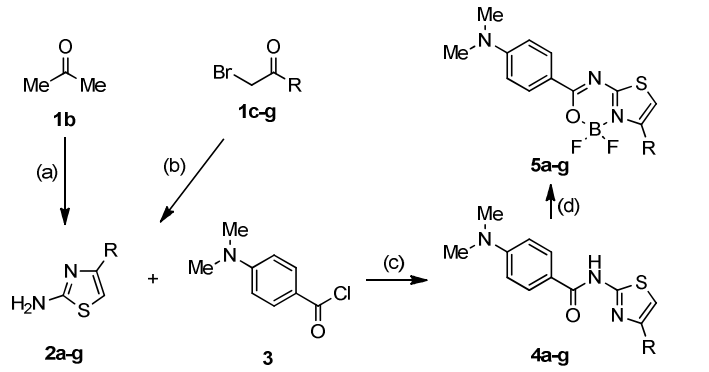

X-Ray Analysis

X-ray analysis of complexes **5a** and **5c–4e** confirmed that, the boron atom is coordinated in a tetrahedral geometry by nitrogen, oxygen and two fluorine atoms. In the solid state, compound **5a** has definitely non-planar geometry. Dimetylaminophenyl group is twisted against thiazolo-oxadiazaborinine unit: the torsion angle of C3−C4−C9−N2 is 24.2° (Figure 1).

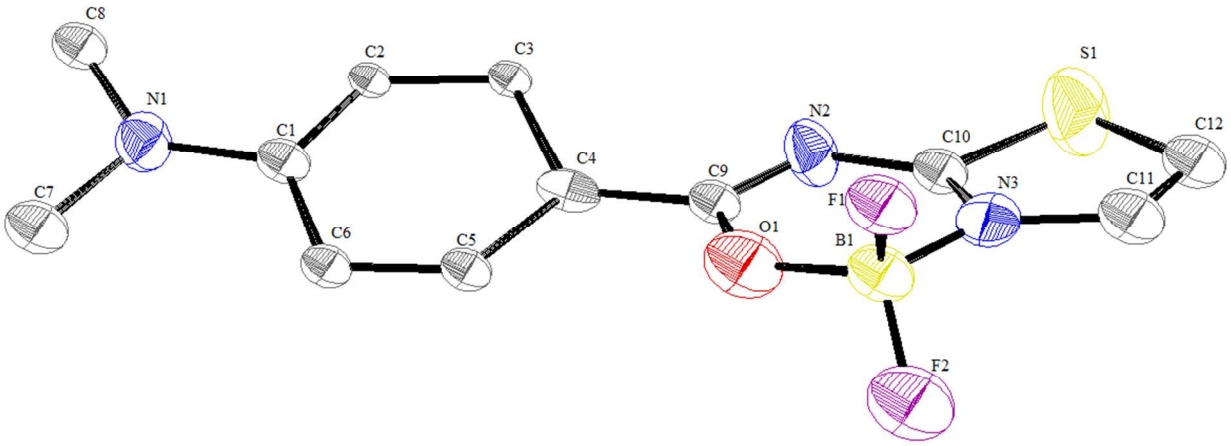

Figure 1. ORTEP diagram of complex **5a**. The ellipsoid contour of probability level is 50%.

On the other hand, complex **5c** exhibits almost planar structure, including ester group at the thiazole unit (the torsion angles of C7−C6−C9−N2 and O2−C13−C10−N3 are 4.0° and 5.1°, respectively) (Figure 2). Another situation is observed in the case of compounds **5d** and **5e**: the main part of the molecules remain flat; however, the aryl substituents at position 4 of thiazole ring are twisted to the rest of the molecules. For complex **5d**, the torsion angles of C16−C11−C10−N2 and C6−C1−C7−N1 are 4.3° and 59.2°. While, the value of the corresponding angles of dye **5e** (C5−C6−C9−N4 and C18−C13−C12−N2) are 3.4° and 58.1°, respectively (Figure 3 and 4).

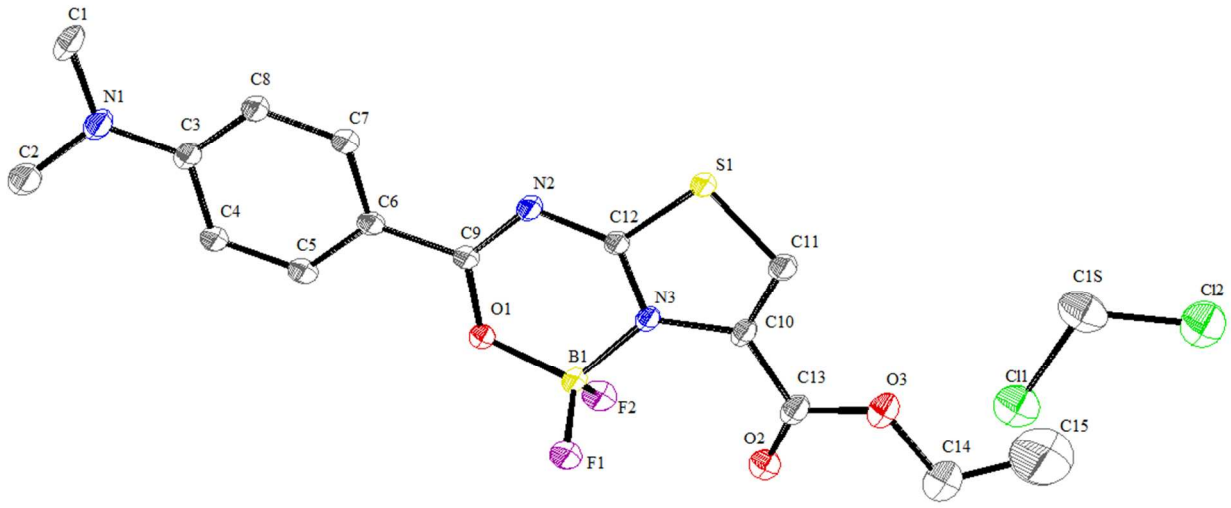

Figure 2. ORTEP diagram of complex **5c**. The ellipsoid contour of probability level is 50%.

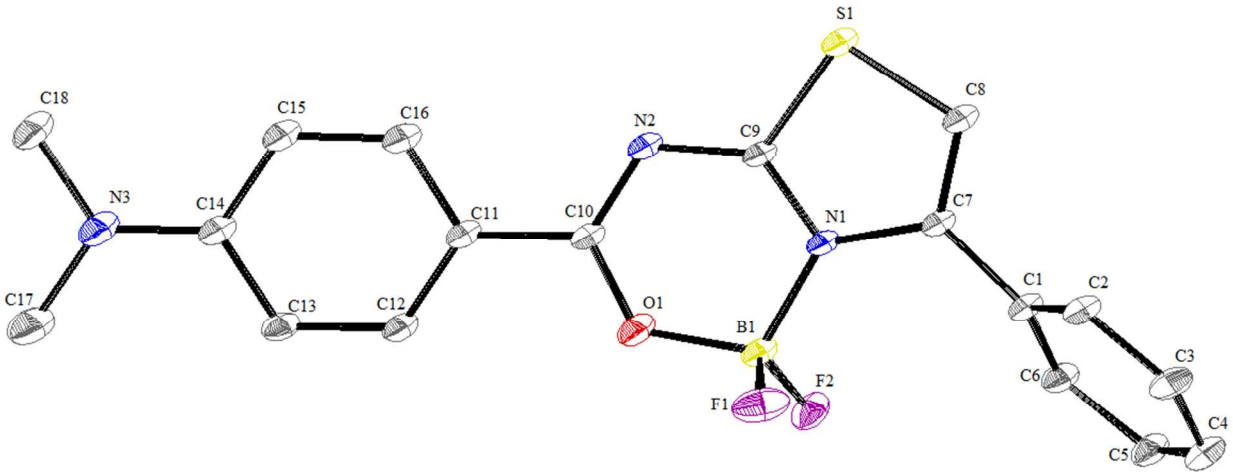

Figure 3. ORTEP diagram of complex **5d**. The ellipsoid contour of probability level is 50%.

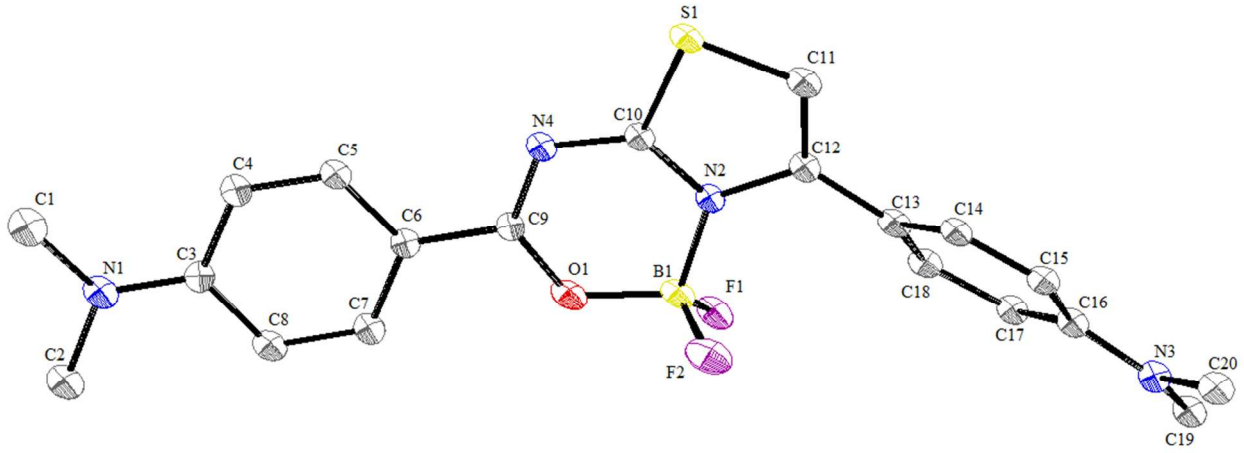

Figure 4. ORTEP diagram of complex **5e**. The ellipsoid contour of probability level is 50%.

Electrochemical Properties

The cyclic voltammetry technique was used to explore the redox behavior of dyes **5a–g**. The oxidation and reduction scans were performed in deoxygenated dichloromethane solution at room temperature with tetrabutylammonium hexafluorophosphate ($TBAPF_6$) as supporting electrolyte. Onset reduction and onset oxidation potentials, as well as, the electron affinities (EAs) and the ionization potentials (IPs) of complexes are summarized in Table 1 and cyclic voltammograms are shown in Figures S1–S7 in the Supporting Information. The values of IP are mostly contained in a narrow range from 5.03 to 5.08 eV; however for compound with additional donor (4-dimethylaminophenyl) substituent at thiazole ring (**5e**) the corresponding value is smaller (4.76 eV). Electron affinity is changing from 2.20–2.35 eV for compounds **5a–d**, and **5f**

to 2.59 eV for **5e**, and is increasing significantly to 2.95 eV for complex with 4-nitrophenyl substituent at thiazole ring (**5g**).

Table 1. Onset Reduction and Onset Oxidation Potentials, Electron Affinities and Ionization Potentials of Complexes 5a–g

Compound	E_{red}^{onset}, V	E_{ox}^{onset}, V	EA, eV	IP, eV
5a	-2.112	0.674	2.29	5.07
5b	-2.203	0.636	2.20	5.04
5c	-2.056	0.663	2.34	5.06
5d	-2.133	0.647	2.27	5.05
5e	-1.810	0.355	2.59	4.76
5f	-2.046	0.676	2.35	5.08
5g	-1.454	0.625	2.95	5.03

Photophysical Characterization of Complexes 5a–g in Solutions

Having established a structural and electrochemical data of boron complexes **5a–g**, we evaluated their photophysical properties. The absorption and fluorescence spectra of the solutions of compounds **5a–g** are demonstrated in Figure 5. The obtained data are summarized in Table S5 in the Supporting Information. The characteristic absorption peak, with the maximum absorption wavelengths at 402–417 nm, showed almost no variation with changing solvent polarity. The molar absorption coefficient values are changed from the minimum for complex **5e** (46,700–50,600 $M^{-1}cm^{-1}$) to maximum for **5g** (60,100–67,600 $M^{-1}cm^{-1}$).

The dilute solutions of **5a–d,f–g** show one very similar emission band centered with the maxima in toluene at 437–448 nm, in DCM at 453–456 nm, in THF at 453–462 nm, and in acetonitrile at 453–477 nm; while compound **5e** is characterized by bathochromic shift (emission maximum in toluene at 518 nm, in DCM at 590 nm, and in THF at 616 nm). In acetonitrile, complex **5e** does not show essential fluorescence. The solvent effect on the fluorescence properties of **5a–g** is manifested in increasing the value of λ_{em} and Stokes shift with the increase of the solvent polarity, while fluorescence quantum yields are decreased. These observations indicate that the fluorescence emission of dyes **5a–g** was partially or fully originated from photoinduced intramolecular charge transfer (ICT) state.

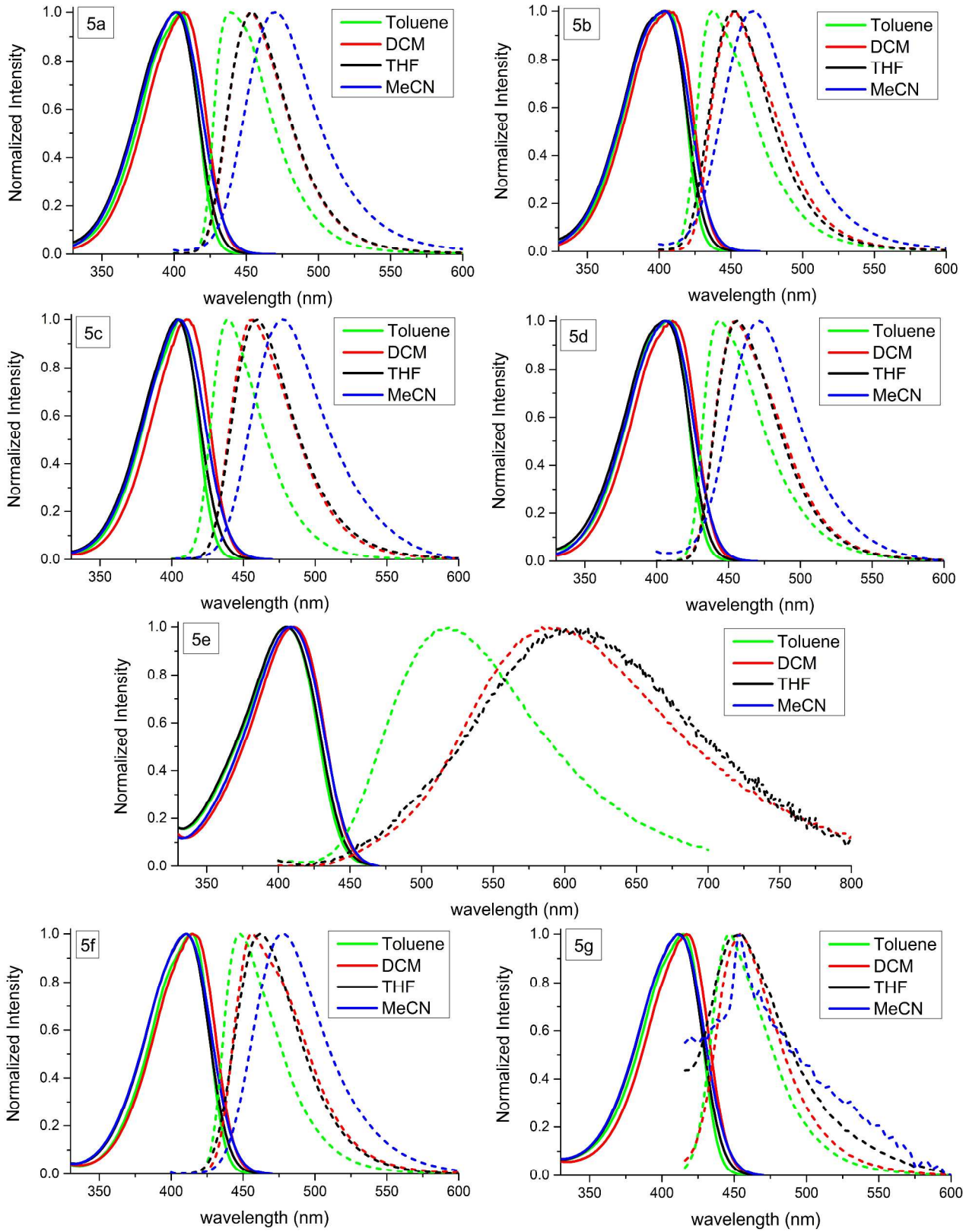

Figure 5. Absorption (solid lines) and emission (dashed lines) spectra of **5a–g** recorded in different solvents

Complexes **5a–d,f** showed very high fluorescent quantum yields in non-polar solvents, while these parameters in acetonitrile are weak. Another properties were observed for complexes **5e** and **5g**. Complex **5e** showed comparatively good quantum yield in toluene (0.66), but very small in DCM, THF and MeCN. Complex **5g** exhibited very weak emission in every investigated solvent. For the THF solutions of the investigated complexes, the lifetimes of excited state were measured (Table 2). It is worth noting that value of the lifetime of compound **5e** (0.21 ns) is considerably smaller that for the rest of complexes (1.39–2.24 ns).

Table 2. Lifetime of the Excited State of Complexes 5a–g in THF

Compound	**5a**	**5b**	**5c**	**5d**	**5e**	**5f**	**5g**
τ, ns	2.22	2.24	2.10	2.06	0.21	1.39	1.64

Quantum Chemical Calculation

To understand the absorption properties of the synthesized complexes, density functional theory (DFT) calculations were performed using the Gaussian 09 software package.[51] All geometrical structures are optimized and molecular orbitals calculated at the B3LYP/6-31G* level. The calculated HOMO-LUMO plots are given in Figure 6.

In compounds **5d–g**, the aryl groups at position 4 of the thiazole ring are twisted in the ground state, what is agreed with X-ray analysis of **5d** and **5e** (Figures 3 and 4). Thus, these substituents are deconjugated with the rest of the molecule. The electron distribution of the HOMOs and LUMOs for **5a–g** is subjected to the general rule that the HOMO electrons are predominantly located on the dimethylaminophenyl group while LUMO electrons are mainly located on thiazolo-oxadiazaborinine moiety. The exceptions are compounds with weak emission properties (**5e** and **5g**). In the case on complex **5e**, there are two donor (dimethylaminophenyl) groups and in HOMO the electron distribution are shifted to donor substituent at thiazole ring, while HOMO-1 is very similar to HOMO of compounds **5a–d** and **5f–g**. The specific situation is observed for compound **5g**: LUMO is shifted from fluorophore unit and preferably located on nitro-phenyl group. However, LUMO+1 has an analogical shape comparably with LUMO of the rest of complexes.

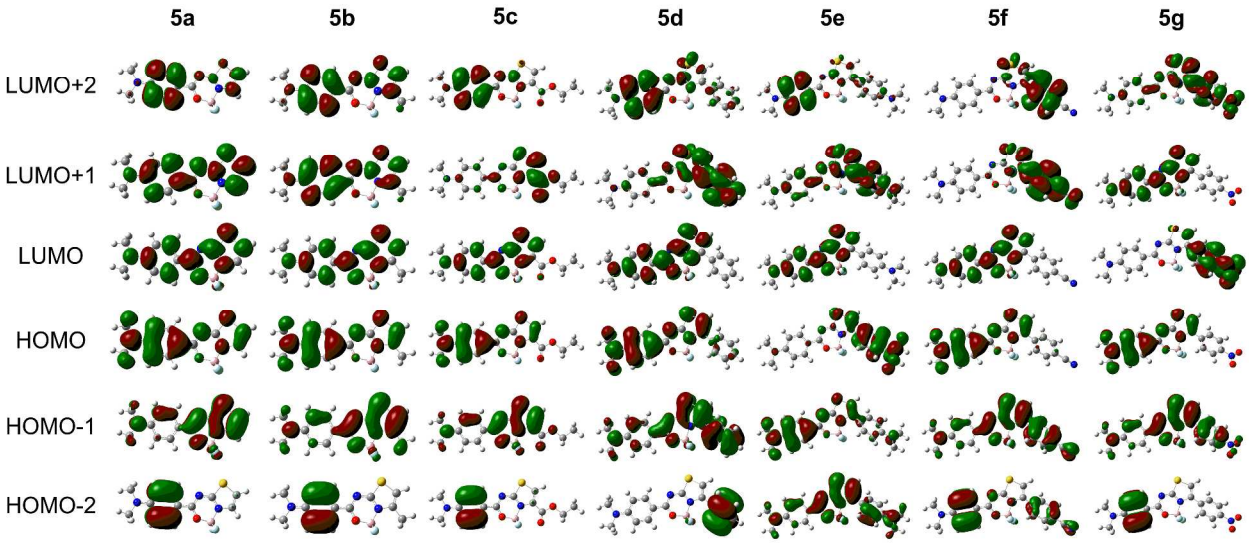

Figure 6. Frontier molecular orbitals of complexes **5a–g**.

To calculate singlet transitions time-dependent DFT (TD-DFT) computations were also performed at the B3LYP/6-31G* level, using previously obtained optimized structures. The calculated excitation energies for the six lowest singlet excited state, maximum absorption wavelengths (λ_{max}), oscillator strengths (*f*) and molecular contribution of the leading configurations are shown in Table S6 in the Supporting Information.

For compounds **5a–d,f** the excitation to the first singlet excited state ($S_0 \rightarrow S_1$) is preferable ($f \sim 1$, λ_{max} = 381–391 nm). Then, these complexes exhibit the reverse transition $S_1 \rightarrow S_0$, which is accompanied by light emission. On the other hand, compound **5e** absorbs light preferably by transition $S_0 \rightarrow S_2$ ($f = 1.1481$, λ_{max} = 380 nm), when electron moves from HOMO-1 to LUMO. For compound **5g**, the excitation also occurs dominantly by $S_0 \rightarrow S_2$ transition ($f = 1.1688$, λ_{max} = 393 nm). However, in this case electron moves from HOMO to LUMO+1. Probably, the de-excitation of molecules **5e** and **5g** includes several transitions ($S_2 \rightarrow S_1$/$S_2 \rightarrow T_1$ and following $S_1 \rightarrow S_0$/$T_1 \rightarrow S_0$), which finally provide to the quenching of fluorescence.

Photophysical Characterization of Complexes 5a–g in the Solid State

To study the solid-state photophysical properties of the synthesized complexes, the thin films were obtained by spin-casting technique from DCM solutions. The emission maxima of the solid samples of all the studied thiazole-boron complexes are red-shifted with respect to those of the corresponding solutions (Figure 7, Table 3). The films of most of the synthesized dyes showed

relatively weak fluorescence quantum yields (Φ = 0.07–0.25), which were apparently predetermined by aggregation induced quenching. Compound **5g** in the solid state as well as in the dilute solution was almost non-emissive (Φ < 0.01). In contrast, the thin film of **5a** exhibited very high fluorescence quantum yield (0.94), which is comparative with that of dilute solutions in nonpolar solvents (toluene, DCM and THF).

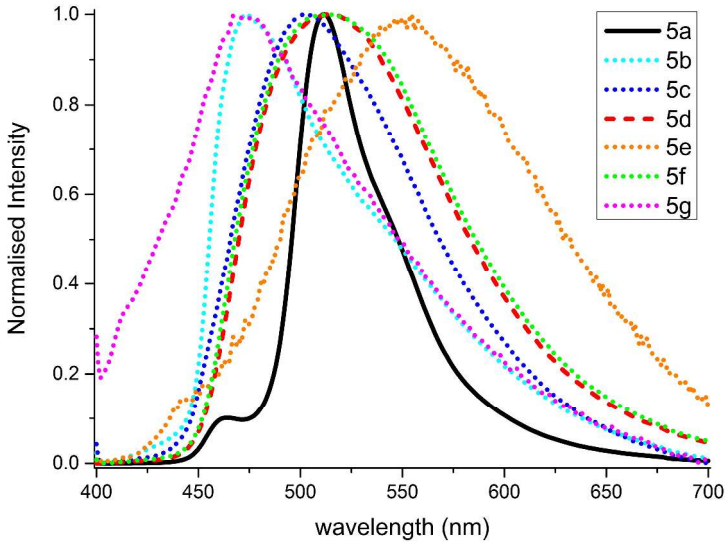

Figure 7. Overlaid normalized emission spectra of **5a–g** in the solid state.

Table 3. Photophysical Data of Complexes 5a–g in the Solid Samples

Compound	λ_{em}, nm	Φ	τ, ns
5a	512	0.94	2.08, 8.83
5b	473	0.12	1.56, 5.66
5c	502	0.09	1.85, 8.79
5d	513	0.25	0.73, 7.51
5e	554	0.10	1.62, 6.11
5f	514	0.07	1.33, 6.35
5g	468	<0.01	1.94, 10.27

The value of fluorescent quantum yield in the solid state largely depends on interactions between the molecules in the crystal packing. In this context, π–π intermolecular interactions can inhibit the fluorescence.[39]

To consider the differences the quantum yield, we carefully analyzed the molecular packing of complexes **5a, c–e**. As shown on Figure 8, molecules **5c** are linked by CH–O (2.93 Å) and CH–F (3.48 Å) hydrogen bonds forming the dimers in the top view. On the other hand, these molecules

are organized in the dimers by π−π and π−n interactions (C−C: 3.43−3.59 Å; C−N: 3.42−3.65 Å) in the side view. Additionally, π−π/π−n interactions were observed for each of these dimers (C−C: 3.41−3.65 Å; C−N: 3.47−3.66 Å), forming stoking columns. Because of the relatively effective π−π/π−n interactions, compound **5c** exhibit weak fluorescent quantum yield (9%) in the solid state.

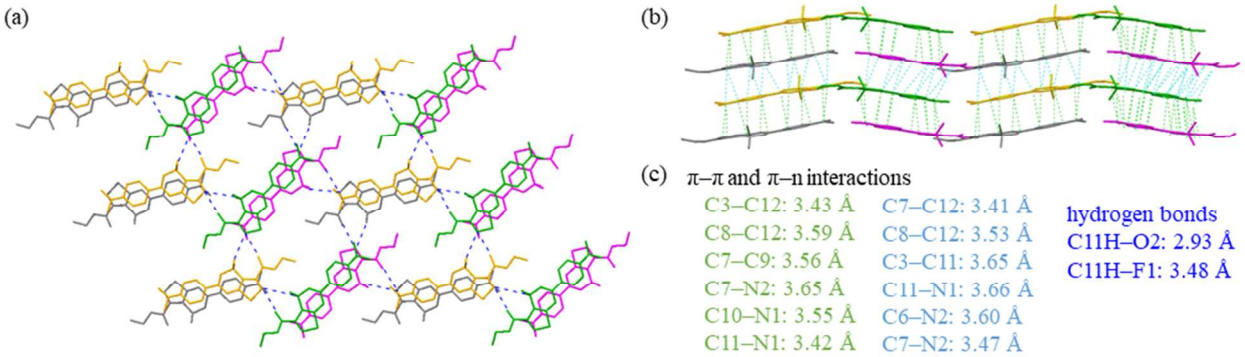

Figure 8. Molecular packing of complex **5c**: (a) top view; (b) side view; (c) list of intermolecular interactions. Green- and light blue-dotted lines show π−π and π−n interactions; blue-dotted lines show hydrogen bonds.

Complex **5e** also exhibits well-ordered packing. The molecules form a net-type structure by connection *via* CH–N (3.50 Å), CH–S (3.80 Å), and two CH–F (3.21 and 3.44 Å) hydrogen bonds. Moreover, the dimethylaminophenyl groups at the position 4 of the thiazole ring demonstrate π−π and π−n interactions (C–C: 3.35–3.59 Å; C–N: 3.36–3.67 Å) (Figure 9). As result, in this case the relatively strong π−π/π−n interactions provide to the weak fluorescence in the solid state (Φ = 10%).

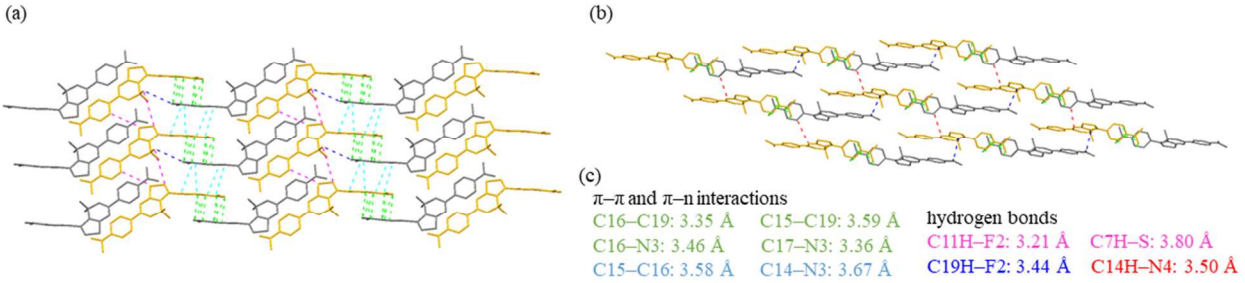

Figure 9. Molecular packing of complex **5e**: (a) top view; (b) side view; (c) list of intermolecular interactions. Green- and light blue-dotted lines show π–π and π–n interactions; magenta-, blue-, and red-dotted lines show hydrogen bonds.

As shown on Figure 10, boron derivative **5d** form layers consisting of dimers interacting *via* a parallel CH–π interactions (CH–C: 3.33–3.49 Å). However, in this structure, effective π–π/π–n interactions do not observed (Figure 12). Therefore, compound **5d** is considered to have weaker intermolecular interactions than **5c** and **5e**, and the slightly higher fluorescent quantum yield of **5d** (Φ = 25%) is probably owing to the non-availability π–π and π–n interactions.

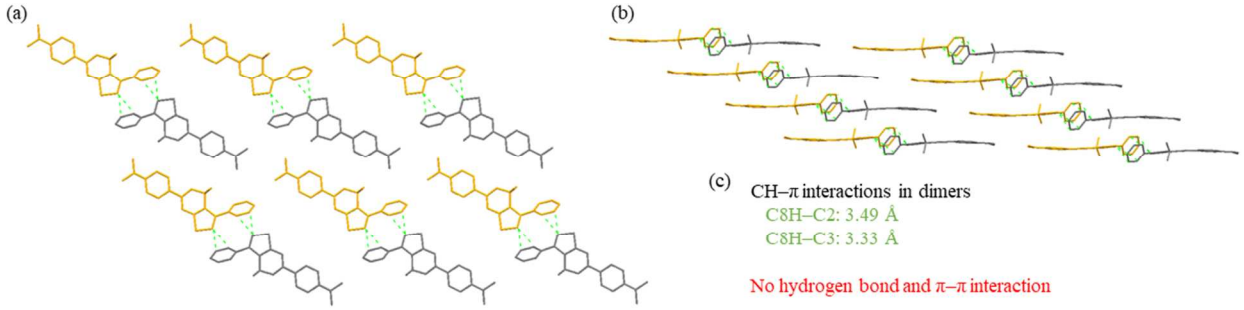

Figure 10. Molecular packing of complex **5d**: (a) top view; (b) side view; (c) list of intermolecular interactions. Green-dotted lines show CH–π interactions in dimers.

For complex **5a**, the molecular packing is definitely different than for dyes **5c–e** (Figure 11). In this case, neighboring molecules are connected by weak CH–F hydrogen bonds (3.04 and 3.31 Å). The dimethylaminophenyl groups are twisted and orientated at some angle towards each other. The molecules do not make any effective π–π or π–n interactions. Because of the inhibition of effective π–π/π–n interactions, the quantum yield of complex **5a** in the solid state is very high (94%).

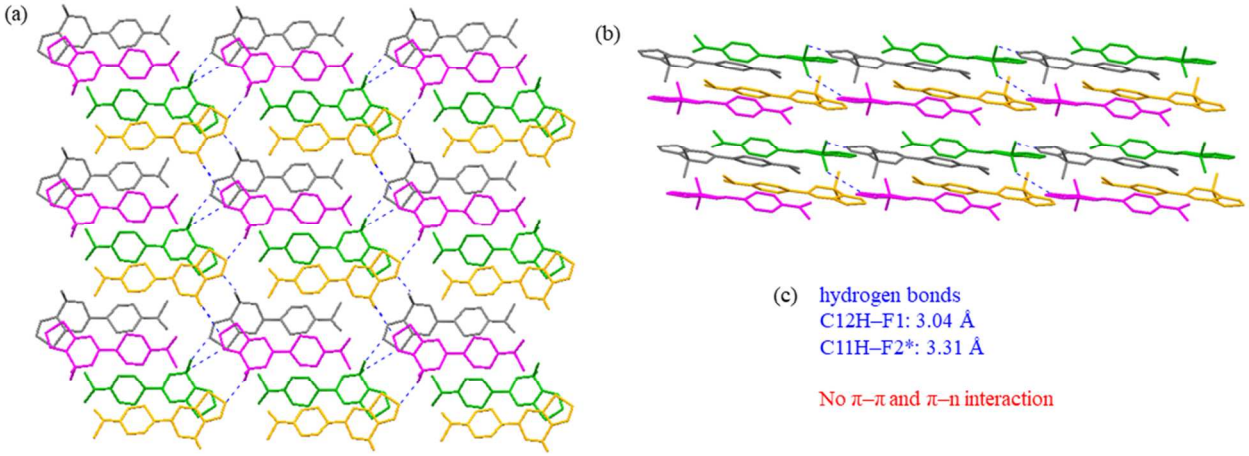

Figure 11. Molecular packing of complex **5a**: (a) top view; (b) side view; (c) list of intermolecular interactions. Blue-dotted lines show hydrogen bonds.

Water-Induced Aggregation of Complexes 4a in THF

Additionally, the fluorescence properties of **5a** were investigated in THF-water mixtures of various ratios (**5a** is soluble in THF but not soluble in water). The fluorescence intensity decreased with increasing water content to 80%. However, when the water content was increased to 90%, the dramatic increase of the fluorescence intensity and the change of emission colour from blue (λ_{em} = 454 nm) to green (λ_{em} = 508 nm) were observed (Figure 12). These changes resulted from the formation of aggregates in the THF-water mixtures, which definitely indicates the effect of aggregation induced emission (AIE)[52] for dye **5a**.

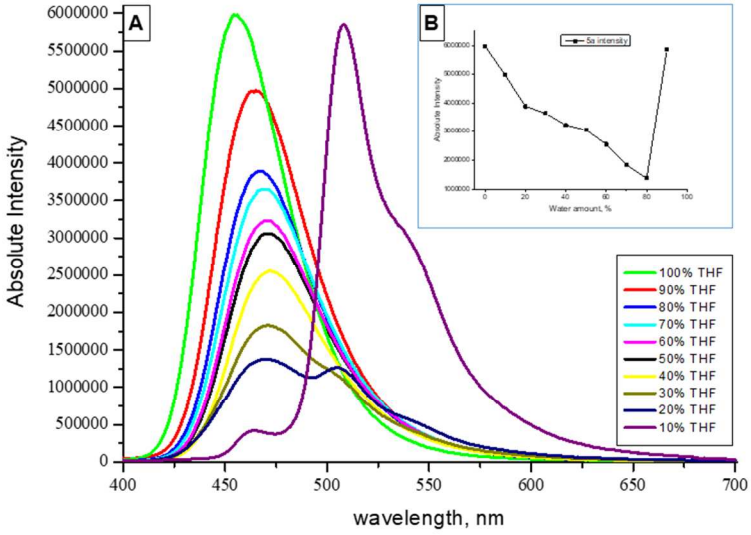

Figure 12. (A) Emission spectra of **5a** in THF/water mixture with different fraction of water and (B) change of emission intensity of **5a** with water fraction.

Analogical investigation of emission activity of complex **5d** (Φ = 25% in the solid state) in THF/H_2O solutions demonstrated missing of the AIE effect (Figure 13). This can by explain by molecular packing. Probably, the reason of the deficiency of AIE effect in this case is formation of the dimer molecules **5d** in the solid state (Figure 10), which is not observed for boron complex **5a** (Figure 11).

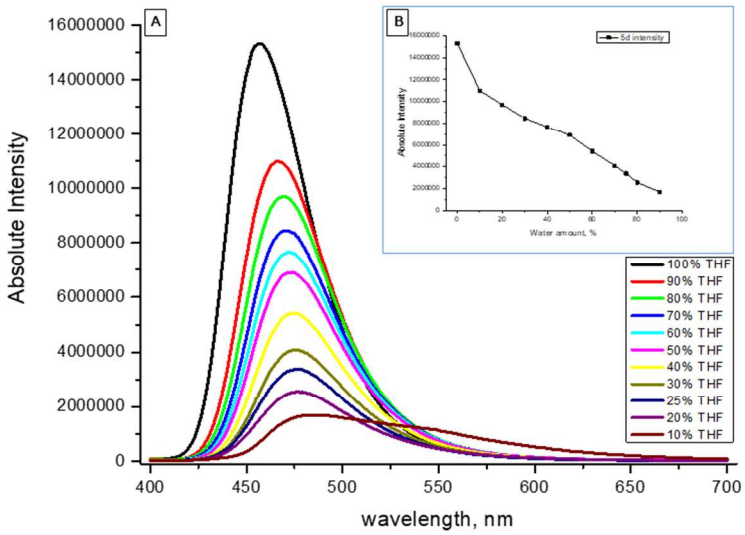

Figure 13. (A) Emission spectra of **5d** in THF/water mixture with different fraction of water and (B) change of emission intensity of **5d** with water fraction.

Conclusions

In conclusion, we developed new *N,O* π-conjugated donor-acceptor organoboron complexes containing thiazole building blocks. Compound with unsubstituted thiazole unit (**5a**) exhibits very high emission in the solutions. The influence of the substitute at position 4 of the thiazole ring on electronic and photophysical properties was investigated. The incorporation of methyl or ethoxycarbonyl groups into the molecular structure (compounds **5b,c**) does not affect significantly on the photophysical parameters in the solution. The aryl groups at position 4 of the thiazole ring are twisted against fluorophore (thiazolo-oxadiazaborinine) unit. As the result, depending on donor/acceptor strength, these substituents can cause the changes in the excitation transitions, which can provide to the fluorescence quenching. In the solid state, most of the synthesized boron complexes showed relatively weak fluorescence quantum yields (7–12%), which were apparently predetermined by aggregation induced quenching. The thin film of complex **5d** exhibited higher fluorescence quantum yield (25%), because of the non-availability π–π and π–n intermolecular interactions in the solid state. In contrast, besause of the unusual molecular packing and inhibition of π–π/π–n interactions, complex **5a** exhibited very high fluorescence quantum yield (94%) in the solid state, and demonstated aggregation induced emission effect.

Experimental Section

General

All chemicals [including 1-(4-(dimethylamino)phenyl)ethan-1-one, ethyl bromopyruvate (**1c**), 2-bromoacetophenone (**1d**), 4-(2-bromoacetyl)benzonitrile (**1f**), 2-bromo-1-(4-nitrophenyl)ethan-1-one (**1g**), and thiazol-2-amine (**2a**)] were received from commercial sources (Aldrich, Alfa Aesar, TCI or Acros Organics) and used without further purification. All reported NMR spectra were recorded with Varian Mercury 400 MHz (at 400 MHz, 100 MHz, and 375 MHz for ^{1}H, ^{13}C, and ^{19}F NMR spectra, respectively), Varian VNMRS 500 MHz (at 500 MHz, 125 MHz, and 470 MHz for ^{1}H, ^{13}C, and ^{19}F NMR spectra, respectively) or Varian VNMRS 600 MHz (at 150 MHz for ^{13}C NMR spectra) spectrometers for solutions in $CDCl_3$ or DMSO-d_6 and TMS as the internal standard. Infrared (IR) spectra were recorded as a solid using attenuated total reflectance (ATR) method or as a film (CH_2Cl_2) with a Jasco FT/IR-6200 spectrometer in the 4000–400 cm^{-1} region. Mass spectra were recorded with Synapt G2-S HDMS (*Waters Inc*) mass spectrometer equipped with an electrospray ion source and q-TOF type mass analyzer. The instrument was controlled and recorded data were processed using *MassLynx V4.1* software package (*Waters Inc*). Thin layer chromatography (TLC) was performed on silica gel plates coated with fluorescent indicator. Colunm chromatography was performed on silica gel (Merck, 230-400 mesh). Melting points were measured on Automatic Melting Point System (OptiMelt, Stanford Research Systems).

UV/Vis spectra of 10^{-5} M solutions of the compounds were recorded in quartz cells using Perkin Elmer Lambda 35 spectrometer. Photoluminescence (PL) spectra of 10^{-5} M solutions of the compounds were recorded using Edinburgh Instruments' FLS980 Fluorescence Spectrometer. Thin solid films for recording of PL spectra were prepared by using spin-coating technique utilizing SPS-Europe Spin150 Spin processor using 2.5 mg/ml solutions of the compounds in DCM on the pre-cleaned quartz substrates. Fluorescence quantum yields of the solutions and of the solid films were estimated using the integrated sphere method. An integrating sphere (Edinburgh Instruments) coupled to the FLS980 spectrometer was calibrated with two standards: quinine sulfate in 0.1 M H_2SO_4 and rhodamine 6G in ethanol. Each quantum yield measurement was repeated 5 times and the error corridor was estimated. Fluorescence decay curves of the samples were recorded using a time-correlated single photon counting technique utilizing the PicoQuant PDL 820 picosecont diode laser as an excitation source. Electrochemical

measurements were carried out using mAUTOLAB Type III apparatus, glassy carbon electrode (diam. 2 mm), platinum coil and silver wire as working, auxiliary and reference electrode, respectively and the scan rate at 100mV/s. Potentials are referenced with respect to ferrocene (Fc), which was used as the internal standard. Cyclic voltammetry experiments were conducted in a standard one-compartment cell, in DMF (Sigma-Aldrich, HPLC grade), under argon. 0.1M Bu_4NPF_6 (Sigma-Aldrich, 99%) was used as the supporting electrolyte. The concentration of compounds was equal 0.1·mmol/dm^3. Deaeration of the solution was achieved by a nitrogen bubbling through the solution for about 10 min before measurement. All electrochemical experiments were carried out under ambient conditions. Ionization potentials (IP) and electron affinities (EA) were determinate from the onset oxidation potentials (E_{ox}^{onset}) and the onset reduction potentials (E_{red}^{onset}), respectively: IP = E_{ox}^{onset} + 4.4; EA = E_{red}^{onset} + 4.4 (Table 1).

X-ray Diffraction

Crystals of compounds **5a** and **5c–e** were obtained by the slow evaporation of their solution in DCM/hexane (1:1). The X-ray measurements were performed at 100 K on SuperNova Agilent *diffractometer* using Mo*K*α (λ = 0.71073 Å) and CuKα (λ = 1.54184 Å) radiation. Data reduction and analysis were carried out with *CrysAlisPro* (Agilent Technologies, *CrysAlisPro, Version 1.171.35.21b).* The structures were solved by direct methods and refined using SHELXL Software Package (Sheldrick, G.M. *Acta Crys*t. 2008, 64a, 112). Crystals of **5a** were of very low quality allowing structure confirmation but not enabling good quality refinement. Crystallographic data for **5a**, **5c–e** have been deposited with the Cambridge Crystallographic Data Centre. Copies of the data can be obtained, free of charge, on application to CCDC, 12 Union Road, Cambridge CB2 1EZ, UK [fax: +44(0)-1223-336033 or e-mail: deposit@ccdc.cam.ac.uk].

Synthesis

4-Methylthiazol-2-amine (2b) was synthesized using a modified literature procedure.[53] To a solution of thiourea (1.00 g, 13.14 mmol) in acetone (1.5 mL) was added iodine (1.67 g, 6.57 mmol) and the reaction mixture was heated under reflux for 4h. After cooling, the solvent was removed by vacuum. The reaction mixture was poured onto ice cold water (15 mL) and adjusted to pH ~ 8 with ammonium hydroxide (25% aqueous solution). The water layer was extracted with ether (5×30 mL), the organic phase was dried (Na_2SO_4) and concentrated. The crude product **2b** was purified by column chromatography (hexanes/AcOEt = 2:1 to 1:2, v/v) to

afford pure yellow oil in 37% yield (0.56 g). ^{1}H NMR (400 MHz, $CDCl_3$): δ = 6.05 (1H, d, *J* = 1.0 Hz, thiazole-H), 5.31 (2H, s, NH_2), 2.21 (3H, d, *J* = 1.0 Hz, CH_3) ppm; ^{13}C NMR (100 MHz, $CDCl_3$): δ = 167.5, 148.5, 102.4, 17.1 ppm. IR (film): 3435, 3294, 3114, 2979, 2949, 2917, 1620, 1520, 1442, 1378, 1332, 1144, 1107, 1035, 969, 841 cm^{-1}.

Synthesis of 4-*R*-thiazol-2-amines 2c,d,f,g (General procedure A) was based on a previous literature procedure.[53] A mixture of 2-halogenoketone **1c,d,f,g** (1 eq.) and thiourea (1 eq.) in ethanol (15 mL) was refluxed for 4h. After cooling, water (30 mL) was added, next, ammonium hydroxide (25% aqueous solution) was added dropwise to pH ~ 8. The product was filtered, dried and used in the next step without further purification.

Ethyl 2-aminothiazole-4-carboxylate (2c) was obtained in 94% yield (523 mg) using general procedure A from ethyl bromopyruvate (**1c**, 628 mg, 3.21 mmol) and thiourea (245 mg, 3.21 mmol). Mp. 142.5–144.2 °C, white powder. ^{1}H NMR (400 MHz, DMSO-d_6): δ = 8.31 (2H, s, NH_2), 7.59 (1H, s, thiazole-H), 4.25 (2H, q, *J* = 7.2 Hz, CH_2), 1.26 (3H, t, *J* = 7.2 Hz, CH_3) ppm; ^{13}C NMR (100 MHz, DMSO-d_6): δ = 168.9, 159.0, 136.0, 117.5, 61.1, 14.1 ppm. IR (film): 3437, 3254, 3125, 2988, 2897, 1691, 1617, 1538, 1368, 1337, 1239, 1076, 1021, 960, 875, 784, 748 cm^{-1}. HRMS (ESI-TOF) calcd for $C_6H_8N_2O_2SNa$ $[M + Na]^+$: 195.0204, found: 195.0197.

4-Phenylthiazol-2-amine (2d) was obtained in 97% yield (431 mg) using general procedure A from 2-bromoacetophenone (**1d**, 500 mg, 2.51 mmol) and thiourea (191 mg, 2.51 mmol). Mp. 149.1–150.3 °C (lit.[54] 150–151 °C), white powder. ^{1}H NMR (400 MHz, DMSO-d_6): δ = 7.79 (2H, d, *J* = 8.0 Hz, Ar-H), 7.35 (2H, dd, *J* = 8.0 Hz, *J* = 7.6 Hz, Ar-H), 7.25 (1H, t, *J* = 7.6 Hz, Ar-H), 7.03 (2H, s, NH_2), 6.98 (1H, s, thiazole-H) ppm; ^{13}C NMR (100 MHz, DMSO-d_6): δ = 168.2, 149.8, 134.9, 128.4 (2C), 127.1, 125.5 (2C), 101.4 ppm. IR (film): 3436, 3255, 3157, 3114, 1596, 1531, 1517, 1482, 1441, 1389, 1332, 1307, 1283, 1200, 1070, 1038, 1021, 909, 845, 771, 713 cm^{-1}. HRMS (ESI-TOF) calcd for $C_9H_9N_2S$ $[M + H]^+$: 177.0486, found: 177.0485.

4-(2-Aminothiazol-4-yl)benzonitrile (2f) was obtained in 98% yield (443 mg) using general procedure A from 4-(2-bromoacetyl)benzonitrile (**1f**, 502 mg, 2.24 mmol) and thiourea (171 mg, 2.24 mmol). Mp. 242.4–244.2 °C, white powder. ^{1}H NMR (400 MHz, DMSO-d_6): δ = 7.96 (2H, d, *J* = 8.4 Hz, Ar-H), 7.80 (2H, d, *J* = 8.4 Hz, Ar-H), 7.29 (1H, s, thiazole-H), 7.16 (2H, s, NH_2) ppm; ^{13}C NMR (100 MHz, DMSO-d_6): δ = 168.5, 148.1, 138.9, 132.5 (2C), 126.1 (2C), 119.0, 109.2, 105.4 ppm. IR (ATR): 3381, 3305, 3115, 2778, 2229, 1644, 1604, 1542, 1482, 1410,

1343, 1284, 1196, 1174, 1133, 1044, 1012, 839, 742, 710 cm^{-1}. HRMS (ESI-TOF) calcd for $C_{10}H_8N_3S$ $[M + H]^+$: 202.0439, found: 202.0435.

4-(4-Nitrophenyl)thiazol-2-amine (2g) was obtained in 93% yield (583 mg) using general procedure A from 2-bromo-1-(4-nitrophenyl)ethan-1-one (**1g**, 505 mg, 2.07 mmol) and thiourea (158 mg, 2.07 mmol). Mp. 284.3–285.7 °C (lit.[54] 285–286 °C), yellow powder. ^{1}H NMR (400 MHz, DMSO-d_6): δ = 8.29 (2H, d, J = 8.8 Hz, Ar-H), 8.01 (2H, d, J = 8.8 Hz, Ar-H), 7.55 (1H, s, thiazole-H), 6.73 (2H, s, NH_2) ppm; ^{13}C NMR (100 MHz, DMSO-d_6): δ = 170.0, 147.0, 139.5, 136.0, 126.8 (2C), 124.2 (2C), 107.3 ppm. IR (ATR): 3399, 3306, 3146, 3115, 1644, 1594, 1539, 1519, 1504, 1411, 1334, 1204, 1110, 1077, 1039, 852, 844, 715 cm^{-1}. HRMS (ESI-TOF) calcd for $C_9H_8N_3O_2S$ $[M + H]^+$: 222.0337, found: 222.0332.

Synthesis of 4-(4-(dimethylamino)phenyl)thiazol-2-amine (2e).

1-(4-(Dimethylamino)phenyl)ethan-1-one (1.00 g, 6.16 mmol) was dissolved in concentrated H_2SO_4 (25 mL) and the solution was cooled to 0 °C. Bromine (0.98 g, 6.16 mmol) was added dropwise over 1h. The reaction mixture was stirred for 2h and poured in ice water (~ 100 mL). Saturated aqueous solution of K_2CO_3 was added to pH ~ 8 and the mixture was extracted with DCM (3×100 mL). The organic layer was dried with Na_2SO_4, filtered, and concentrated. The resulting crude product was purified by column chromatography (hexanes/ethyl acetate = 9:1, v/v) to give 2-bromo-1-(4-(dimethylamino)phenyl)ethan-1-one (**1e**) (1.28 g, 86%). Mp. 90.5–92.1 °C (lit.[55] 91–92 °C), green powder. ^{1}H NMR (400 MHz, $CDCl_3$): δ = 7.88 (2H, d, J = 8.9 Hz, Ar-H), 6.65 (2H, d, J = 8.9 Hz, Ar-H), 4.35 (2H, s, CH_2), 3.07 (6H, s, 2 × CH_3) ppm; ^{13}C NMR (100 MHz, $CDCl_3$): δ = 189.3, 153.8, 131.3 (2C), 121.7, 110.7 (2C), 40.0 (2C), 30.7 ppm.

2-Bromo-1-(4-(dimethylamino)phenyl)ethan-1-one (**1e**, 700 mg, 2.89 mmol) was dissolved in EtOH (30 mL). Thiourea (220 mg, 2.89 mmol) was added and the reaction mixture was refluxed for 4h. After cooling, ethanol was removed by vacuum. The reaction mixture was poured onto ice cold water (15 mL) and adjusted to pH ~ 8 with ammonium hydroxide (25% aqueous solution). The water layer was extracted with DCM (3×30 mL), the organic phase was dried (Na_2SO_4) and concentrated. The product **2e** was purified by column chromatography (DCM/MeOH = 100:0 to 99:1, v/v) to afford solid in 68% yield (430 mg). Mp. 188.0–190.3 °C, yellow powder. ^{1}H NMR (400 MHz, DMSO-d_6): δ = 7.61 (2H, d, J = 8.9 Hz, Ar-H), 6.90 (2H, br s, NH_2), 6.69 (2H, d, J = 8.9 Hz, Ar-H), 6.65 (1H, s, thiazole-H), 2.91 (6H, s, 2 × CH_3) ppm; ^{13}C NMR (100 MHz, DMSO-d_6): δ = 167.8, 150.4, 149.5, 126.4 (2C), 123.5, 112.0 (2C), 97.3, 40.0

(2C) ppm. IR (ATR): 3456, 3357, 3264, 3118, 3090, 2925, 2806, 1638, 1609, 1542, 1514, 1496, 1442, 1359, 1336, 1228, 1199, 1168, 1126, 1065, 1040, 1002, 946, 817, 736 cm^{-1}. HRMS (ESI-TOF) calcd for $C_{11}H_{14}N_3S$ $[M + H]^+$: 220.0908, found: 220.0909.

Synthesis of ligands 4a–g (General procedure B). To a solution of amine **2a–g** in 1,4-dioxane (20 mL) were added 4-(dimethylamino)benzoyl chloride (**3**, 1 eq.), distillated trimethylamine (3 eq.) and DMAP (0.05 eq.). The reaction mixture was refluxed for 24h. After cooling, a saturated aqueous solution (50 mL) of $NaHCO_3$ were added and the mixture was extracted with DCM (3 × 40 mL). The combined organic layers were dried over Na_2SO_4, filtered and concentrated. The product was purified by column chromatography (DCM/MeOH = 100:0 to 99:1, v/v).

4-(Dimethylamino)-*N*-(thiazol-2-yl)benzamide (4a) was obtained in 72% yield (105 mg) using general procedure B from **2a** (59 mg, 0.59 mmol) and **3** (108 mg, 0.59 mmol). Mp. 163.0–165.2 °C, white powder. ^{1}H NMR (400 MHz, $CDCl_3$): δ = 12.33 (1H, s, NH), 7.97 (2H, d, *J* = 9.0 Hz, Ar-H), 7.25 (1H, d, *J* = 3.8 Hz, thiazole-H), 6.91 (1H, d, *J* = 3.8 Hz, thiazole-H), 6.70 (2H, d, *J* = 9.0 Hz, Ar-H), 3.06 (6H, s, 2 × CH_3) ppm; ^{13}C NMR (100 MHz, $CDCl_3$): δ = 165.4, 160.9, 153.2, 136.9, 129.8 (2C), 118.8, 112.8, 111.1 (2C), 40.0 (2C) ppm. IR (ATR): 3300, 3159, 2938, 1655, 1601, 1535, 1440, 1374, 1320, 1286, 1194, 1167, 1127, 1062, 944, 891 829, 745 cm^{-1}. HRMS (ESI-TOF) calcd for $C_{12}H_{13}N_3OSNa$ $[M + Na]^+$: 270.0677, found: 270.0672.

4-(Dimethylamino)-*N*-(4-methylthiazol-2-yl)benzamide (4b) was obtained in 66% yield (115 mg) using general procedure B from **2b** (76 mg, 0.67 mmol) and **3** (122 mg, 0.67 mmol). Mp. 214.4–216.1 °C, white powder. ^{1}H NMR (400 MHz, $CDCl_3$): δ = 10.88 (1H, s, NH), 7.81 (2H, d, *J* = 9.0 Hz, Ar-H), 6.66 (2H, d, *J* = 9.0 Hz, Ar-H), 6.50 (1H, d, *J* = 1.0 Hz, thiazole-H), 3.04 (6H, s, 2 × CH_3), 2.15 (3H, d, *J* = 1.0 Hz, thiazole-CH_3) ppm; ^{13}C NMR (100 MHz, $CDCl_3$): δ = 164.8, 159.3, 153.2, 146.9, 129.4 (2C), 118.6, 111.0 (2C), 107.8, 40.0 (2C), 16.80 ppm. IR (film): 2921, 2812, 1653, 1604, 1526, 1442, 1371, 1290, 1195, 1135, 1064, 978, 944, 895, 827, 758, 724 cm^{-1}. HRMS (ESI-TOF) calcd for $C_{13}H_{15}N_3OSNa$ $[M + Na]^+$: 284.0834, found: 284.0829.

Ethyl 2-(4-(dimethylamino)benzamido)thiazole-4-carboxylate (4c) was obtained in 46% yield (117 mg) using general procedure B from **2c** (138 mg, 0.80 mmol) and **3** (147 mg, 0.80 mmol). Mp. 163.5–165.2 °C, white powder. ^{1}H NMR (400 MHz, $CDCl_3$): δ = 10.03 (1H, s, NH), 7.84 (1H, s, thiazole-H), 7.80 (2H, d, *J* = 9.2 Hz, Ar-H), 6.69 (2H, d, *J* = 9.2 Hz, Ar-H), 4.33 (2H, q, *J*

= 7.2 Hz, CH_2), 3.06 (6H, s, 2 × CH_3), 1.36 (3H, t, *J* = 7.2 Hz, $CH_2C\underline{H_3}$) ppm; ^{13}C NMR (100 MHz, $CDCl_3$): δ = 164.6, 161.6, 159.0, 153.4, 141.6, 129.2 (2C), 122.1, 117.5, 111.1 (2C), 61.3, 40.0 (2C), 14.3 ppm. IR (film): 3115, 2930, 1717, 1655, 1604, 1529, 1442, 1370, 1330, 1290, 1198, 1136, 1096, 1022, 945, 898, 826, 756 cm^{-1}. HRMS (ESI-TOF) calcd for $C_{15}H_{17}N_3O_3SNa$ $[M + Na]^+$: 342.0888, found: 342.0880.

4-(Dimethylamino)-*N*-(4-phenylthiazol-2-yl)benzamide (4d) was obtained in 70% yield (133 mg) using general procedure B from **2d** (103 mg, 0.58 mmol) and **1** (107 mg, 0.58 mmol). Mp. 195.0–196.4 °C, white powder. ^{1}H NMR (400 MHz, $CDCl_3$): δ = 10.00 (1H, s, NH), 7.80 (2H, d, *J* = 8.0 Hz, Ar-H), 7.77 (2H, d, *J* = 8.8 Hz, Ar-H), 7.37 (2H, dd, *J* = 7.2 Hz, *J* = 8.0 Hz, Ar-H), 7.27 (2H, t, *J* = 7.2 Hz, Ar-H), 7.13 (1H, s, thiazole-H), 6.60 (2H, d, *J* = 8.8 Hz, Ar-H), 3.01 (6H, s, 2 × CH_3) ppm; ^{13}C NMR (100 MHz, $CDCl_3$): δ = 164.5, 159.0, 153.2, 149.9, 134.5, 129.1 (2C), 128.6 (2C), 127.8, 126.0 (2C), 118.0, 111.0 (2C), 107.6, 39.9 (2C) ppm. IR (film): 3234, 3106, 3059, 2915, 1653, 1604, 1526, 1482, 1442, 1372, 1327, 1282, 1197, 1173, 1137, 1062, 1027, 946, 893, 825, 776, 758, 722 cm^{-1}. HRMS (ESI-TOF) calcd for $C_{18}H_{18}N_3OS$ $[M + H]^+$: 324.1171, found: 324.1167.

4-(Dimethylamino)-*N*-(4-(4-(dimethylamino)phenyl)thiazol-2-yl)benzamide (4e) was obtained in 80% yield (148 mg) using general procedure B from **2e** (110 mg, 0.50 mmol) and **3** (110 mg, 0.50 mmol). Mp. 209.4–211.0 °C, green powder. ^{1}H NMR (400 MHz, $CDCl_3$): δ = 9.99 (1H, s, NH), 7.83 (2H, d, *J* = 9.0 Hz, Ar-H), 7.69 (2H, d, *J* = 8.8 Hz, Ar-H), 6.91 (1H, s, thiazole-H), 6.73 (2H, d, *J* = 8.8 Hz, Ar-H), 6.66 (2H, d, *J* = 9.0 Hz, Ar-H), 3.03 (6H, s, 2 × CH_3), 2.97 (6H, s, 2 × CH_3) ppm; ^{13}C NMR (100 MHz, $CDCl_3$): δ = 164.3, 158.7, 153.2, 150.4, 150.3, 139.1 (2C), 127.0 (2C), 123.3, 118.4, 112.4 (2C), 111.2 (2C), 104.4, 40.4 (2C), 40.0 (2C) ppm. IR (ATR): 3108, 2896, 2803, 1649, 1609, 1524, 1495, 1441, 1368, 1331, 1283, 1231, 1197, 1133, 1064, 947, 892, 823, 758 cm^{-1}. HRMS (ESI-TOF) calcd for $C_{20}H_{23}N_4OS$ $[M + H]^+$: 367.1593, found: 367.1593.

***N*-(4-(4-Cyanophenyl)thiazol-2-yl)-4-(dimethylamino)benzamide (4f)** was obtained in 50% yield (87 mg) using general procedure B from **2f** (100 mg, 0.50 mmol) and **3** (91 mg, 0.50 mmol). Mp. 230.1–232.4 °C, yellow powder. ^{1}H NMR (400 MHz, $CDCl_3$): δ = 9.96 (1H, s, NH), 7.87 (2H, d, *J* = 8.6 Hz, Ar-H), 7.79 (2H, d, *J* = 9.0 Hz, Ar-H), 7.61 (2H, d, *J* = 8.6 Hz, Ar-H), 7.27 (1H, s, thiazole-H), 6.64 (2H, d, *J* = 9.0 Hz, Ar-H), 3.05 (6H, s, 2 × CH_3) ppm; ^{13}C NMR (100 MHz, $CDCl_3$): δ = 164.5, 159.5, 153.3, 147.9, 138.5, 132.4 (2C), 129.2 (2C), 126.4

(2C), 118.9, 117.7, 111.0 (2C), 111.0, 110.5, 40.0 (2C) ppm. IR (ATR): 3340, 3105, 2925, 2856, 2226, 1748, 1655, 1608, 1532, 1445, 1374, 1323, 1278, 1194, 1091, 1056, 944, 890, 850, 825, 752, 712 cm^{-1}. HRMS (ESI-TOF) calcd for $C_{19}H_{16}N_4OSNa$ $[M + Na]^+$: 371.0943, found: 371.0936.

4-(Dimethylamino)-*N*-(4-(4-nitrophenyl)thiazol-2-yl)benzamide (4g) was obtained in 62% yield (113 mg) using general procedure B from **2g** (110 mg, 0.50 mmol) and **3** (91 mg, 0.50 mmol). Mp. 276.2–277.1 °C, yellow powder. ^{1}H NMR (400 MHz, DMSO-d_6): δ = 12.39 (1H, s, NH), 8.29 (2H, d, *J* = 8.0 Hz, Ar-H), 8.19 (2H, d, *J* = 8.0 Hz, Ar-H), 8.04 (2H, d, *J* = 8.4 Hz, Ar-H), 7.94 (1H, s, thiazole-H), 6.75 (2H, d, *J* = 8.4 Hz, Ar-H), 3.01 (6H, s, 2 × CH_3) ppm; ^{13}C NMR (100 MHz, DMSO-d_6): δ = 164.8, 159.6, 153.0, 146.7, 146.3, 140.5, 129.8 (2C), 126.5 (2C), 124.1 (2C), 117.6, 112.5, 110.8 (2C), 39.6 (2C) ppm. IR (ATR): 3426, 3104, 2907, 2819, 1645, 1603, 1526, 1505, 1433, 1371, 1333, 1269, 1190, 1108, 1060, 945, 873, 824, 758, 726 cm^{-1}. HRMS (ESI-TOF) calcd for $C_{18}H_{17}N_4O_3S$ $[M + H]^+$: 369.1021, found: 369.1014.

Synthesis of complexes 5a–g (General procedure C). To a solution of compound **4a–g** in dry DCM (20 mL) were added $BF_3 \cdot Et_2O$ (10 eq.) and distillated *N*,*N*-diisopropylethylamine (20 eq.) under an argon atmosphere. The reaction mixture was stirred for 24h at room temperature and then washed with water. The organic phase was dried over anhydrous Na_2SO_4, and filtered. The solvent was removed under reduced pressure and the crude product was purified by column chromatography (hexanes/dichloromethane from 1:1 to 0:1, v/v).

4-(1,1-Difluoro-1*H*-1λ^4,8λ^4-thiazolo[3,2-*c*][1,3,5,2]oxadiazaborinin-3-yl)-*N*,*N*-dimethylaniline (5a) was obtained in 58% yield (51 mg) using general procedure C from ligand **4a** (74 mg, 0.30 mmol). Mp. 245.2–246.8 °C, yellow powder. ^{1}H NMR (400 MHz, $CDCl_3$): δ = 8.18 (2H, d, *J* = 9.2 Hz, Ar-H), 7.46 (1H, d, *J* = 4.4 Hz, thiazole-H), 6.95 (1H, d, *J* = 4.4 Hz, thiazole-H), 6.67 (2H, d, *J* = 9.2 Hz, Ar-H), 3.09 (6H, s, 2 × CH_3) ppm; ^{13}C NMR (100 MHz, $CDCl_3$): δ = 173.9, 167.0, 154.2, 132.3 (2C), 129.6, 117.4, 112.3, 110.9 (2C), 40.0 (2C) ppm; ^{19}F NMR (375 MHz, $CDCl_3$): δ = –136.63 (d, *J* = 11.4 Hz), –136.69 (d, *J* = 11.4 Hz) ppm. IR (film): 3156, 3121, 2920, 2852, 1615, 1556, 1538, 1499, 1463, 1423, 1363, 1276, 1227, 1183, 1127, 1063, 940, 911, 874, 860, 820, 761, 724, 702 cm^{-1}. HRMS (ESI-TOF) calcd for $C_{12}H_{12}BN_3OF_2SNa$ $[M + Na]^+$: 318.0660, found: 318.0654.

4-(1,1-Difluoro-7-methyl-1*H*-1λ^4,8λ^4-thiazolo[3,2-*c*][1,3,5,2]oxadiaza-borinin-3-yl)-*N*,*N*-dimethylaniline (5b) was obtained in 51% yield (48 mg) using general procedure C from ligand

4b (79 mg, 0.30 mmol). Mp. 224.0–226.3 °C, yellow powder. ^{1}H NMR (400 MHz, $CDCl_3$): δ = 8.18 (2H, d, *J* = 9.2 Hz, Ar-H), 6.67 (2H, d, *J* = 9.2 Hz, Ar-H), 6.50 (1H, d, *J* = 0.7 Hz, thiazole-H), 3.08 (6H, s, 2 × CH_3), 2.49 (3H, d, *J* = 0.7 Hz, thiazole-CH_3) ppm; ^{13}C NMR (100 MHz, $CDCl_3$): δ = 173.6, 166.2, 154.1, 141.9, 132.2 (2C), 117.5, 110.9 (2C), 106.9, 40.0 (2C), 14.9 ppm; ^{19}F NMR (375 MHz, $CDCl_3$): δ = –133.77 (d, *J* = 13.0 Hz), –133.84 (d, *J* = 13.0 Hz) ppm. IR (film): 3114, 2911, 1609, 1573, 1567, 1488, 1451, 1402, 1370, 1285, 1227, 1192, 1135, 1056, 1000, 929, 897, 850, 822, 743, 708 cm^{-1}. HRMS (ESI-TOF) calcd for $C_{13}H_{15}BN_3OF_2S$ $[M + H]^+$: 310.0997, found: 310.0991.

Ethyl 3-(4-(dimethylamino)phenyl)-1,1-difluoro-1*H*-1*λ*^{4},8*λ*^{4}-thiazolo[3,2-*c*][1,3,5,2]oxadiazaborinine-7-carboxylate (5c) was obtained in 48% yield (51 mg) using general procedure C from ligand **4c** (92 mg, 0.29 mmol). Mp. 193.6–195.4 °C, yellow powder. ^{1}H NMR (500 MHz, $CDCl_3$): δ = 8.19 (2H, d, *J* = 9.2 Hz, Ar-H), 7.75 (1H, s, thiazole-H), 6.67 (2H, d, *J* = 9.2 Hz, Ar-H), 4.43 (2H, q, *J* = 7.5 Hz, CH_2), 3.10 (6H, s, 2 × CH_3), 1.42 (3H, t, *J* = 7.2 Hz, CH_3) ppm; ^{13}C NMR (125 MHz, $CDCl_3$): δ = 174.8, 167.1, 157.3, 154.4, 136.2, 132.7 (2C), 120.5, 116.7, 110.9 (2C), 62.3, 40.0 (2C), 14.0 ppm; ^{19}F NMR (470 MHz, $CDCl_3$): δ = –131.57 (d, *J* = 6.6 Hz), –131.63 (d, *J* = 10.8 Hz) ppm. IR (film): 3133, 2922, 1730, 1606, 1562, 1530, 1495, 1455, 1407, 1369, 1288, 1218, 1190, 1131, 1058, 930, 822, 757, 734 cm^{-1}. HRMS (ESI-TOF) calcd for $C_{15}H_{17}BN_3O_3F_2S$ $[M + H]^+$: 368.1052, found: 368.1043.

4-(1,1-Difluoro-7-phenyl-1*H*-1*λ*^{4},8*λ*^{4}-thiazolo[3,2-*c*][1,3,5,2]oxadiaza-borinin-3-yl)-*N*,*N*-dimethylaniline (5d) was obtained in 58% yield (64 mg) using general procedure C from ligand **4d** (96 mg, 0.30 mmol). Mp. 221.1–222.4 °C, yellow powder. ^{1}H NMR (400 MHz, $CDCl_3$): δ = 8.18 (2H, d, *J* = 9.2 Hz, Ar-H), 7.68 (2H, dd, *J* = 8.4 Hz, *J* = 2.0 Hz, Ar-H), 7.43–7.48 (3H, m, Ar-H), 6.76 (1H, s, thiazole-H), 6.67 (2H, d, *J* = 9.2 Hz, Ar-H), 3.07 (6H, s, 2 × CH_3) ppm; ^{13}C NMR (100 MHz, $CDCl_3$): δ = 174.2, 166.3, 154.2, 146.1, 132.3 (2C), 131.0, 126.2 (2C, t, $J_{C\text{-}F}$ = 5.6 Hz), 129.1, 128.3 (2C), 117.3, 110.9 (2C), 109.1, 40.0 (2C) ppm; ^{19}F NMR (375 MHz, $CDCl_3$): δ = –130.47 (d, *J* = 10.0 Hz), –130.53 (d, *J* = 10.0 Hz) ppm. IR (film): 3136, 2923, 1610, 1562, 1543, 1480, 1404, 1369, 1334, 1286, 1227, 1186, 1137, 1046, 934, 886, 823, 751 cm^{-1}. HRMS (ESI-TOF) calcd for $C_{18}H_{16}BN_3OF_2SK$ $[M + K]^+$: 410.0712, found: 410.0704.

4,4'-(1,1-Difluoro-1*H*-1*λ*^{4},8*λ*^{4}-thiazolo[3,2-*c*][1,3,5,2]oxadiazaborinine-3,7-diyl)bis(*N*,*N*-dimethylaniline) (5e) was obtained in 77% yield (89 mg) using general procedure C from ligand **4e** (102 mg, 0.28 mmol). Mp. 206.2–208.4 °C, yellow powder. ^{1}H NMR (500 MHz, $CDCl_3$): δ =

8.19 (2H, d, J = 9.2 Hz, Ar-H), 7.58 (2H, d, J = 8.9 Hz, Ar-H), 6.75 (2H, d, J = 8.9 Hz, Ar-H), 6.67 (2H, d, J = 9.2 Hz, Ar-H), 6.65 (1H, s, thiazole-H), 3.08 (6H, s, 2 × CH_3), 3.01 (6H, s, 2 × CH_3) ppm; ^{13}C NMR (125 MHz, $CDCl_3$): δ = 173.9, 165.9, 154.0, 151.0, 147.0, 132.2 (2C), 130.0 (2C), 118.5, 117.5, 111.5 (2C), 110.9 (2C), 107.2, 40.2 (2C), 40.1 (2C) ppm; ^{19}F NMR (470 MHz, $CDCl_3$): δ = –130.50 (d, J = 10.1 Hz), –130.55 (d, J = 8.8 Hz) ppm. IR (film): 2893, 2808, 1609, 1560, 1484, 1445, 1404, 1368, 1338, 1228, 1195, 1137, 1048, 942, 927, 888, 822, 756 cm^{-1}. HRMS (ESI-TOF) calcd for $C_{20}H_{22}BN_4OF_2S$ [M + H]$^+$: 415.1575, found: 415.1576.

4-(3-(4-(Dimethylamino)phenyl)-1,1-difluoro-1*H*-1λ^4,8λ^4-thiazolo[3,2-*c*][1,3,5,2]oxadiazaborinin-7-yl)benzonitrile (5f) was obtained in 56% yield (43 mg) using general procedure C from ligand **4f** (67 mg, 0.19 mmol). Mp. 197.4–199.1 °C, yellow powder. ^{1}H NMR (500 MHz, $CDCl_3$): δ = 8.19 (2H, d, J = 9.0 Hz, Ar-H), 7.82 (2H, d, J = 8.0 Hz, Ar-H), 7.75 (2H, d, J = 8.0 Hz, Ar-H), 6.87 (1H, s, thiazole-H), 6.68 (2H, d, J = 9.0 Hz, Ar-H), 3.10 (6H, s, 2 × CH_3) ppm; ^{13}C NMR (125 MHz, $CDCl_3$): δ = 174.6, 166.6, 154.4, 143.8, 135.3, 132.6 (2C), 132.2 (2C), 129.8 (2C), 118.3, 116.8, 113.4, 110.9 (2C), 110.6, 40.1 (2C) ppm; ^{19}F NMR (470 MHz, $CDCl_3$): δ = –129.97 (d, J = 10.3 Hz), –130.02 ppm. IR (film): 3105, 2917, 2224, 1606, 1556, 1483, 1455, 1403, 1372, 1335, 1191, 1155, 1137, 1100, 1038, 948, 930, 882, 859, 832, 761, 736, 711 cm^{-1}. HRMS (ESI-TOF) calcd for $C_{19}H_{15}BN_4OF_2SNa$ [M + Na]$^+$: 419.0925, found: 419.0916.

4-(1,1-Difluoro-7-(4-nitrophenyl)-1*H*-1λ^4,8λ^4-thiazolo[3,2-*c*][1,3,5,2]-oxadiazaborinin-3-yl)-*N*,*N*-dimethylaniline (5g) was obtained in 68% yield (61 mg) using general procedure C from ligand **4g** (79 mg, 0.21 mmol). Mp. 201.3–203.6 °C, orange powder. ^{1}H NMR (400 MHz, $CDCl_3$): δ = 8.31 (2H, d, J = 8.8 Hz, Ar-H), 8.19 (2H, d, J = 9.2 Hz, Ar-H), 7.89 (2H, d, J = 8.8 Hz, Ar-H), 6.91 (1H, s, thiazole-H), 6.68 (2H, d, J = 9.2 Hz, Ar-H), 3.11 (6H, s, 2 × CH_3) ppm; ^{13}C NMR (150 MHz, $CDCl_3$): δ = 174.7, 166.7, 154.4, 148.4, 143.4, 137.0, 132.6 (2C), 130.2 (2C), 123.6 (2C), 116.8, 111.0 (2C), 110.9, 40.1 (2C) ppm; ^{19}F NMR (375 MHz, $CDCl_3$): δ = –129.89 (d, J = 9.8 Hz), –129.96 (d, J = 9.8 Hz) ppm. IR (film): 3115, 2918, 1609, 1552, 1519, 1463, 1406, 1374, 1345, 1284, 1232, 1193, 1139, 1058, 946, 929, 890, 854, 823, 742 cm^{-1}. HRMS (ESI-TOF) calcd for $C_{18}H_{16}BN_4O_3F_2S$ [M + H]$^+$: 417.1004, found: 417.0996.

Keywords: boron complex • 1,3-thiazole • thiazolo[3,2-c][1,3,5,2]oxadiazaborinine • aggregation induced emission (AIE) • fluorescence

ASSOCIATED CONTENT

Supporting Information

The Supporting Information is available free of charge *via* the Internet at http://pubs.acs.org at DOI:

ORTEP diagrams for the X-ray structures **5a**, **5c–5e**; crystal data of complexes **5a**, **5c–e**; cyclic voltammograms of **5a–g**; photophysical properties of complexes **5a–g** in different solvents; fluorescence decays of dyes **5a–g**; calculated properties of the 6 lowest singlet excited states for complexes **5a–g** determined through TD-DFT; optimized geometry for compounds **5a–g**; NMR spectra; IR spectra.

AUTHOR INFORMATION

Corresponding Author

*E-mail: potopnyk@gmail.com

ORCID

Mykhaylo A. Potopnyk: 0000-0002-4543-2785

ACKNOWLEDGMENTS

This work was financially supported by the Research Council of Lithuania (project No TAP LU-2-2016).

REFERENCES

(1) Yang, X.; Zhou, G.; Wong, W.-Y. *Chem. Soc. Rev.* **2015**, *44*, 8484.

(2) Furue, R.; Nishimoto, T.; Park, I. S.; Lee, J.; Yasuda, T. *Angew. Chem. Int. Ed.* **2016**, *55*, 7171.

(3) Li, X.-L.; Xie, G.; Liu, M.; Chen, D.; Cai, X.; Peng, J.; Cao, Y.; Su, S.-J. *Adv. Mater.* **2016**, *28*, 4614.

(4) Liu, Y.; Xie, G.; Wu, K.; Luo, Z.; Zhou, T.; Zeng, X.; Yu, J.; Gong, S.; Yang, C. *J. Mater. Chem. C* **2016**, *4*, 4402.

(5) Ganschow, M.; Koser, S.; Hahn, S.; Rominger, F.; Freudenberg, J.; Bunz, U. H. F. *Chem. Eur. J.* **2017**, *23*, 4415.

(6) Costa, R. D.; Ortí, E.; Bolink, H. J.; Monti, F.; Accorsi, G.; Armaroli, N. *Angew. Chem. Int. Ed.* **2012**, *51*, 8178.

(7) Subeesh, M. S.; Shanmugasundaram, K.; Sunesh, C. D.; Nguyen, T. P.; Choe, Y. *J. Phys. Chem. C* **2015**, *119*, 23676.

(8) Fernández, A.; Vendrell, M. *Chem. Soc. Rev.* **2016**, *45*, 1182.

(9) Un, H.-I.; Wu, S.; Huang, C.-B.; Xu, Z.; Xu, L. *Chem. Commun.* **2015**, *51*, 3143.

(10) de Moliner, F.; Kielland, N.; Lavilla, R.; Vendrell, M. *Angew. Chem. Int. Ed.* **2017**, *56*, 3758.

(11) Sahoo, S. K.; Sharma, D.; Bera, R. K.; Crisponi, G.; Callan, J. F. *Chem. Soc. Rev.* **2012**, *41*, 7195.

(12) Song, N.; Chen, D.-X.; Xia, M.-C.; Qiu, X.-L.; Ma, K.; Xu, B.; Tian, W.; Yang, Y.-W. *Chem. Commun.* **2015**, *51*, 5526.

(13) Causa, F.; Aliberti, A.; Cusano, A. M.; Battista, E.; Netti, P. A. *J. Am. Chem. Soc.* **2015**, *137*, 1758.

(14) Loudet, A.; Burgess, K. *Chem. Rev.* **2007**, *107*, 4891.

(15) Kowada, T.; Maeda, H.; Kikuchi, K. *Chem. Soc. Rev.* **2015**, *44*, 4953.

(16) Zhao, J.; Xu, K.; Yang, W.; Wang, Z.; Zhong, F. *Chem. Soc. Rev.* **2015**, *44*, 8904.

(17) Frath, D.; Massue, J.; Ulrich, G.; Ziessel, R. *Angew. Chem. Int. Ed.* **2014**, *53*, 2290.

(18) Glotzbach, C.; Kauscher, U.; Voskuhl, J.; Kehr, N. S.; Stuart, M. C. A.; Fröhlich, R.; Galla, H. J.; Ravoo, B. J.; Nagura, K.; Saito, S.; Yamaguchi, S.; Würthwein, E.-U. *J. Org. Chem.* **2013**, *78*, 4410.

(19) Marks, T.; Daltrozzo, E.; Zumbusch, A. *Chem. Eur. J.* **2014**, *20*, 6494.

(20) Gao, N.; Cheng, C.; Yu, C.; Hao, E.; Wang, S.; Wang, J.; Wei, Y.; Mu, X.; Jiao, L. *Dalton Trans.* **2014**, *43*, 7121.

(21) Liu, Q.; Wang, X.; Yan, H.; Wu, Y.; Li, Z.; Gong, S.; Liu, P.; Liu, Z. *J. Mater. Chem. C* **2015**, *3*, 2953.

(22) Cheng, C.; Gao, N.; Yu, C.; Wang, Z.; Wang, J.; Hao, E.; Wei, Y.; Mu, X.; Tian, Y.; Ran, C.; Jiao, L. *Org. Lett.* **2015**, *17*, 278.

(23) Shimizu, S.; Murayama, A.; Haruyama, T.; Iino, T.; Mori, S.; Furuta, H.; Kobayashi, N. *Chem. Eur. J.* **2015**, *21*, 12996.

(24) Yang, C.; Wang, X.; Wang, M.; Xu, K.; Xu, C. *Chem. Eur. J.* **2017**, *23*, 4310.

(25) Bukowska, P.; Piechowska, J.; Loska, R. *Dyes and Pigments* **2017**, 137, 312.

(26) Kwak, M. J.; Kim, Y. *Bull. Korean Chem. Soc.* **2009**, *30*, 2865.

(27) Zhou, Y.; Kim, J. W.; Nandhakumar, R.; Kim, M. J.; Cho, E.; Kim, Y. S.; Jang, Y. H.; Lee, C.; Han, S.; Kim, K. M.; Kim, J.-J.; Yoon, J. *Chem. Commun.* **2010**, *46*, 6512.

(28) Murale, D. P.; Lee, K. M.; Kim, K.; Churchill, D. G. *Chem. Commun.* **2011**, *47*, 12512.

(29) Santra, M.; Moon, H.; Park, M.-H.; Lee, T.-W.; Kim, Y. K.; Ahn, K. H. *Chem. Eur. J.* **2012**, *18*, 9886.

(30) Massue, J.; Frath, D.; Ulrich, G.; Retailleau, P.; Ziessel, R. *Org. Lett.* **2012**, *14*, 230.

(31) Frath, D.; Azizi, S.; Ulrich, G.; Ziessel, R. *Org. Lett.* **2012**, *14*, 4774.

(32) Benelhadj, K.; Massue, J.; Retailleau, P.; Ulrich, G.; Ziessel, R. *Org. Lett.* **2013**, *15*, 2918.

(33) Massue, J.; Frath, D.; Retailleau, P.; Ulrich, G.; Ziessel, R. *Chem. Eur. J.* **2013**, *19*, 5375.

(34) Chen, Y.; Qi, D.; Zhao, L.; Cao, W.; Huang, C.; Jiang, J. *Chem. Eur. J.* **2013**, *19*, 7342.

(35) Li, X.; Son, Y.-A. *Dyes and Pigments* **2014**, *107*, 182.

(36) Zhang, P.; Liu, W.; Niu, G.; Xiao, H.; Wang, M.; Ge, J.; Wu, J.; Zhang, H.; Li, Y.; Wang, P. *J. Org, Chem.* **2017**, *82*, 3456.

(37) Kubota, Y.; Niwa, T.; Jin, J.; Funabiki, K.; Matsui, M. *Org, Chem.* **2015**, *17*, 3174.

(38) Kubota, Y.; Tanaka, S.; Funabiki, K.; Matsui, M. *Org. Lett.* **2012**, *14*, 4682.

(39) Kubota, Y.; Ozaki, Y.; Funabiki, K.; Matsui, *J. Org. Chem.* **2013**, *78*, 7058.

(40) Ośmiałowski, B.; Zakrzewska, A.; Jędrzejewska, B.; Grabarz, A.; Zaleśny, R.; Bartkowiak, W.; Kolehmainen, E. *J. Org. Chem.* **2015**, *80*, 2072.

(41) Grabarz, A. M.; Jędrzejewska, B.; Zakrzewska, A.; Zaleśny, R.; Laurent, A. D.; Jacquemin, D.; Ośmiałowski, B. *J. Org. Chem.* **2017**, *82*, 1529.

(42) Kubota, Y.; Kasatani, K.; Takai, H.; Funabiki, K.; Matsui, M. *Dalton Trans.* **2015**, *44*, 3326.

(43) Du, M.-L.; Hu, C.-Y.; Wang, L.-F.; Li, C.; Han, Y.-Y.; Gan, X.; Chen, Y.; Mu, W.-H.; Huang, M. L.; Fu, W.-F. *Dalton Trans.* **2014**, *43*, 13924.

(44) Wu, Y.-Y.; Chen, Y.; Gou, G.-Z.; Mu, W.-H.; Lv, X.-J.; Du, M.-L.; Fu, W.-F. *Org. Lett.* **2012**, *14*, 5226.

(45) Wu, G. F.; Xu, Q. L.; Guo, L. E.; Zang, T. N.; Tan, R.; Tao, S. T.; Ji, J. F.; Hao, R. T.; Zhang, J. F.; Zhou, Y. *Tetrahedron Lett.* **2015**, *56*, 5034.

(46) Grabarz, A. M.; Laurent, A. D.; Jędrzejewska, B.; Zakrzewska, A.; Jacquemin, D.; Ośmiałowski, B. *J. Org. Chem.* **2016**, *81*, 2280.

(47) Bednarska, J.; Zaleśny, R.; Wielgus, M.; Jędrzejewska, B.; Puttreddy, R.; Rissanen, K.; Bartkowiak, W.; Ågren, H.; Ośmiałowski, B. *Phys. Chem. Chem. Phys.* **2017**, *19*, 5705.

(48) Fin, A.; Jentzsch, A.V.; Sakai, N.; Matile, S. *Angew. Chem. Int. Ed.* **2012**, *51*, 12736.

(49) Szymański, W.; Wu, B.; Poloni, C.; Janssen, D. B.; Feringa, B. L. *Angew. Chem. Int. Ed.* **2013**, *52*, 2068.

(50) Diac, A.; Demeter, D.; Allain, M.; Grosu, I.; Roncali, J. *Chem. Eur. J.* **2015**, *21*, 1598.

(51) Frisch, M. J.; Trucks, G. W.; Schlegel, H. B.; Scuseria, G. E.; Robb, M. A.; Cheeseman, J. R.; Scalmani, G.; Barone, V.; Mennucci, B.; Petersson, G. A.; Nakatsuji, H.; Caricato, M.; Li, X.; Hratchian, H. P.; Izmaylov, A. F.; Bloino, J.; Zheng, G.; Sonnenberg, J. L.; Hada, M.; Ehara, M.; Toyota, K.; Fukuda, R.; Hasegawa, J.; Ishida, M.; Nakajima, T.; Honda, Y.; Kitao, O.; Nakai, H.; Vreven, T.; Montgomery, J. A., Jr.; Peralta, J. E.; Ogliaro, F.; Bearpark, M.; Heyd, J. J.; Brothers, E.; Kudin, K. N.; Staroverov, V. N.; Keith, T.; Kobayashi, R.; Normand, J.; Raghavachari, K.; Rendell, A.; Burant, J. C.; Iyengar, S. S.; Tomasi, J.; Cossi, M.; Rega, N.; Millam, J. M.; Klene, M.; Knox, J. E.; Cross, J. B.; Bakken, V.; Adamo, C.; Jaramillo, J.; Gomperts, R.; Stratmann, R. E.; Yazyev, O.; Austin, A. J.; Cammi, R.; Pomelli, C.; Ochterski, J. W.; Martin, R. L.; Morokuma, K.; Zakrzewski, V. G.; Voth, G. A.; Salvador, P.; Dannenberg, J. J.; Dapprich, S.; Daniels, A. D.; Farkas, O.; Foresman, J. B.; Ortiz, J. V.; Cioslowski, J.; Fox, D. J. *Gaussian 09*, revision D.01; Gaussian, Inc.: Wallingford, CT, USA, 2013.

(52) Mei, J.; Leung, N. L. C.; Kwok, R. T. K.; Lam, J. W. Y.; Tang, B. Z. *Chem. Rev.* **2015**, *115*, 11718.

(53) Huang, G.; Sun, H.; Qiu, X.; Jin, C.; Lin, C.; Shen, Y.; Jiang, J.; Wang, L. *Org. Lett.* **2011**, *13*, 5224.

(54) Yan, G.; Hao, L.; Niu, Y.; Huang, W.; Wang, W.; Xu, F.; Liang, L.; Wang, C.; Jin, H.; Xu, P. *Eur. J. Med. Chem.* **2017**, *137*, 462.

(55) Diwu, Z.; Beachdel, C.; Klaubert, D. H. *Tetrahedron Lett.* **1998**, *39*, 4987.